Journal of Energy Technologies and Policy
ISSN 2224-3232 (Paper) ISSN 2225-0573 (Online)
Vol.7, No.6, 2017
www.iiste.org

Experimental Investigation of the Thermal Buoyancy Characteristics of a Mixed Mode Natural Convection Solar Crop Dryer with Back Up Heater

C.K.K. Sekyere[1*] F.W. Adam[2a] F. Davis[2b] F.K., Forson[2c]
1. Department of Mechanical and Manufacturing Engineering, University of Energy and Natural Resources P.O. Box 214, Sunyani, Ghana
2. Department of Mechanical Engineering, Kwame Nkrumah University of Science and Technology, Kumasi, Ghana

The research was solely financed by the authors

Abstract
An experimental investigation into the thermal buoyancy characteristics of a mixed-mode natural convection solar crop dryer with back up heater is described. Twenty seven carefully planned tests were conducted under no load conditions for plenum inlet gap to vent outlet gap ratios of 1:1, 1:1.3 and 1:1.5, in order to determine the optimum thermal drive characteristics of the dryer. Air velocities, temperatures, ambient relative humidity, collector efficiency, exergy rate of change, thermal mass entropy change and air mass flow rate are presented. The effects of the various plenum inlet and vent outlet gap configurations described above on dryer thermal buoyancy are deduced and discussed. Results show that for all heating modes, an air inlet gap to vent gap ratio of 1.5:1 optimises the thermal performance of the dryer.
Keywords: Solar dryer, back up heater, exergy, plenum, thermal mass

Nomenclature

A	Cross sectional area of flow passage (m^2)
C_p	Specific heat capacity at constant pressure (J/kg.K)
C_v	Specific heat capacity at constant volume (J/kg.K)
g	Acceleration due to gravity (m/s^2)
h	Specific enthalpy of air (kJ/kg)
H	Height (m)
K	Loss coefficient
$\dot{m}_o$	Mass flow rate of air (kg/s)
P	Pressure (hPa)
$\dot{Q}_{tm}$	Thermal mass heat absorption rate (W)
R	Specific gas constant of air (kJ/kg.K)
s	Specific entropy (kJ/kg. K)
$\overline{S}_c$	Radiant energy incident on cover glass (W/m^2)
T	Temperature (^oC)
V	Local wind speed (m/s)
z	Altitude with respect to back up heater housing floor (m)
β	Bulk coefficient of expansion (K^{-1})
η_c	Air-heater efficiency (%)
ϕ	Relative humidity (%)
ρ	Average air density (kg/m^3)
$\Delta\dot{\psi}$	Rate of change of flow exergy (kW)

Subscripts

ab	absorber;	db	drying bed unit;	rp-bh	rock pile-back up heater interface
bu	back up heater unit;	fi	fluid inlet;	rp-f	rock pile-fluid interface
cu	collector unit;	fo	fluid outlet;	vu	vent outlet unit
cp	plenum cover glass;	i	inlet	dc	drying chamber cover glass;
				o	outlet

1. Introduction

Sun drying is currently the commonest mode of drying in Ghana. Sun drying refers to spreading the products to be dried on the concrete floor, table, cloth or any other available surface and leaving it in the open space to be

dried by the sun. In Ghana, this inefficient traditional drying technique is used by the rural and commercial farmers to dry about 90 % of the total agricultural produce (Dapaah, 1991). Most farmers cannot afford to import expensive mechanical drying equipment, which is either electricity or diesel engine-powered, with the additional financial burden of maintenance and other running expenses. Though the traditional method of drying crops is cheap and environmentally friendly, it is labour intensive, and requires a large area of land to dry a relatively small quantity of crop. In addition, the method provides no control over the drying process and no crop protection against unexpected rain and/or strong wind, Furthermore, the crop being dried is subject to contamination by dirt and infestation by insects, rodents, moulds, and pests (Ratti and Mujumdar, 1997). All these problems result in a poor quality dried product and in post-harvest losses (for example, in Ghana the figure can be as high as 20 to 30 %). The economic consequences to the farmer and to the country arising from these losses can be substantial (Dapaah, 1991). Some of the problems associated with open sun drying can be solved through the use of solar dryers (Soponronnarit, 1995). The solar dryer is controlled environment which may be made of a combination of glazing and wood or glazing and brick with nets at air inlet and air outlet. Solar dryers are less labour intensive, have high temperatures, and can produce low relative humidity heated air which improves the rate of drying and results in lower final moisture content of the produce which is the most important factor that can affect the growth of micro-organisms in stored grains and agricultural products. Nevertheless, one disadvantage of solar drying is that the dehydration process is interrupted and is slowed down at night and there can be re-absorption of water by the partially dried products resulting in the dried product being of poor quality (Madhlopa et al, 2006). A natural convection solar dryer is very appropriate for use in areas where electricity is not available. Among the different types of natural convection solar dryers, the mixed-mode type has been demonstrated to be superior in the speed of drying (Simate, 2003).

When using the sun's radiation as the energy source for drying, two principal difficulties must be overcome in order to exploit the full potential of solar dryers: the periodic character and the time dependence of the solar radiation. The influence of weather changes must also be considered.

The periodic character of the solar radiation can partly be balanced by employing an intermittent drying operation. However, because the number of hours of available sunshine is very much dependent on the prevalent weather conditions, the use of a heat storage unit may be needed. The dependence of the dryer performance on the weather, especially in large systems, should be minimised by providing an auxiliary energy source. This auxiliary energy source is connected to the dryer by means of a heat exchanger and operates in emergency situations only.

2.0 Description and operation of dryer

Experiments were carried out on a laboratory model of the system. The laboratory model was adopted in order to cut down on the cost of experimentation. Figures 1, 2, and 3, show sketches of the dryer and solar simulator unit, the concrete absorber and rock pebble bed unit, and the vent outlet openings integrated into the dryer hardware to control the outflow of air.

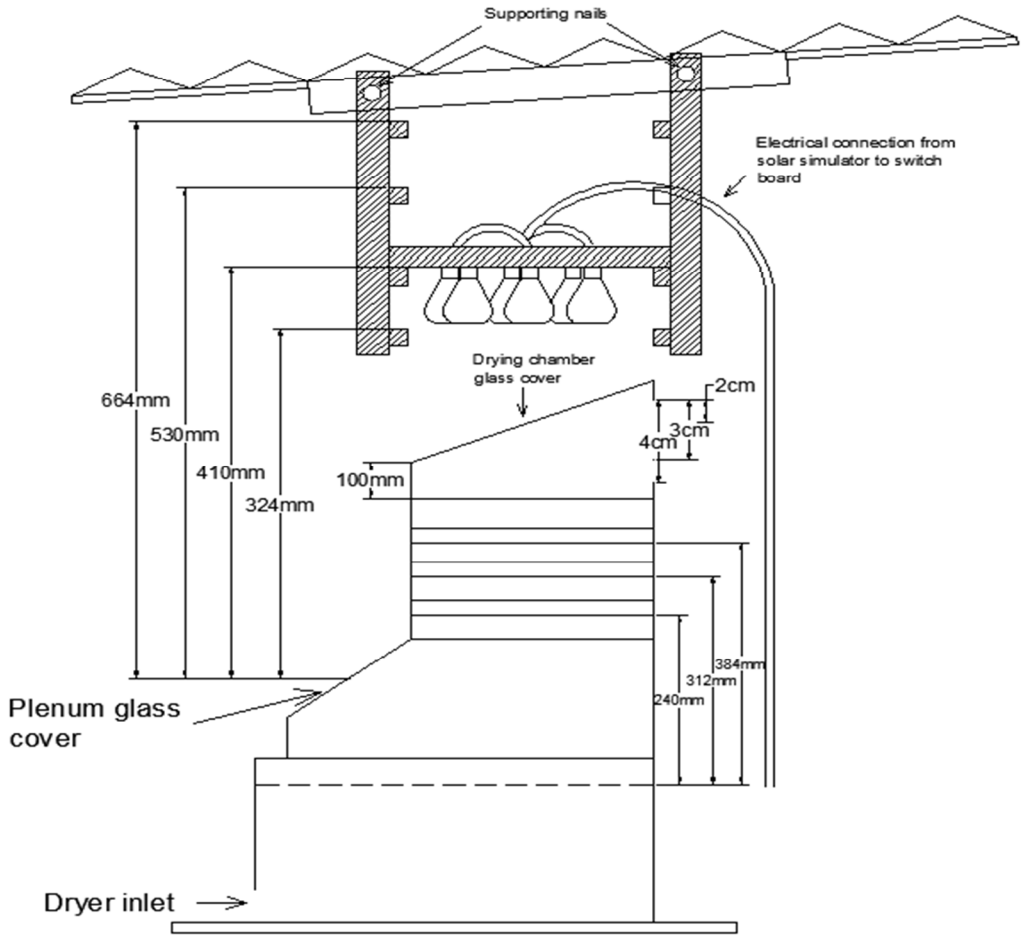

Figure 1 Solar dryer and solar simulator arrangement

Six infra-red lamps, 120 W each, arranged on a panel which could be fixed at four different heights (324 mm, 410 mm, 530 mm, and 664 mm) above the middle plane of the plenum glass cover, as shown in figure 1 are collectively used to simulate the incident solar energy required for the drying operation.

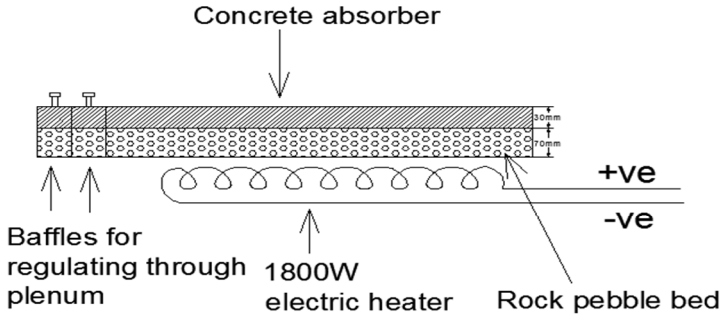

Figure 2 Concrete absorber and rock pebble bed arrangement

The main components of the dryer are: an1800 Watt electric resistance heater attached to the base of the thermal mass (shown in figure 2)*; a drying chamber*, in which the product to be dried is placed; and *a vent*, through which the moist air is vented to the surrounding.

The thermal mass system which measures 400 mm × 275 mm × 100 mm was painted matt black on its top surface to improve its thermal absorptivity. The plenum air inlet opening (31 cm by length internal) has two centimeter (2 cm) thick baffles (shown in figure 3) for regulating air flow through the dryer. The rectangular air gap was adjusted to 20, 40, and 60 mm widths. The rock bed made up 70 mm thickness of the integrated concrete absorber thermal mass and had a rock pebble volume of 0.00355 m^3 whereas the concrete absorber was 30 mm thick.

Figure 3 Integrated absorber-thermal mass system showing slabs for controlling air flow

The *drying chamber* has a trapezoidal section but with a rectangular drying surface measuring 141 mm x 367 mm. It houses three removable extended metal-mesh trays, arranged vertically in line on guides that are spaced 72 mm apart with the lower tray at a height of 240 mm from the base of the plenum. The second and third trays as shown in figure 1 are 312 mm and 376 mm from the plenum base, respectively. The distance from the top of the third tray to the lower edge of the drying chamber roof is 100 mm. The side walls are made up of block board and the roof is made of glazing. There is a door that provides access to the chamber for loading, and unloading the crop and it measures 200 mm × 402 mm. The entire wooden structure that makes up the plenum and drying chamber fits into a rectangular slot (measuring 440 mm × 425 mm internally) with a glass foil insulation material between the wooden components of the system and the heater compartment

The dryer is designed to operate with solar radiation as the main energy source. The back-up heater is used when radiation is inadequate and at night so that continuous drying is not interrupted. When the dryer is run on solar energy, atmospheric air picks up heat energy absorbed by the concrete absorber and rises through the drying cabinet to effect drying. In addition, direct solar radiation entering through the transparent top cover, is absorbed by the interior surfaces of the cabinet and by the crop, thus, providing additional energy for drying. The heated surfaces further warm the surrounding air, which rises by natural convection, passing through the drying trays and picking up moisture from the product being dried. The moist air finally exits the dryer through the vents on the upper back side of the cabinet. This action reduces the pressure inside the cabinet and ambient air is drawn into the dryer through the inlet holes in the brick wall. A continuous flow of air is thus established.

During periods of low radiation, the back-up heater is used to supply the extra heat energy for drying. The resistance heater heats up the rock pile bottom surface, which in turn warms the air naturally aspirated through the system as it moves over the rock pile surface. The warm air rises up into the drying chamber, evaporating and picking up the crop moisture as it passes through the trays, and then escapes through the top vents as before. By regulating the amount of air entering the back up heater the heat delivery rate can be controlled.

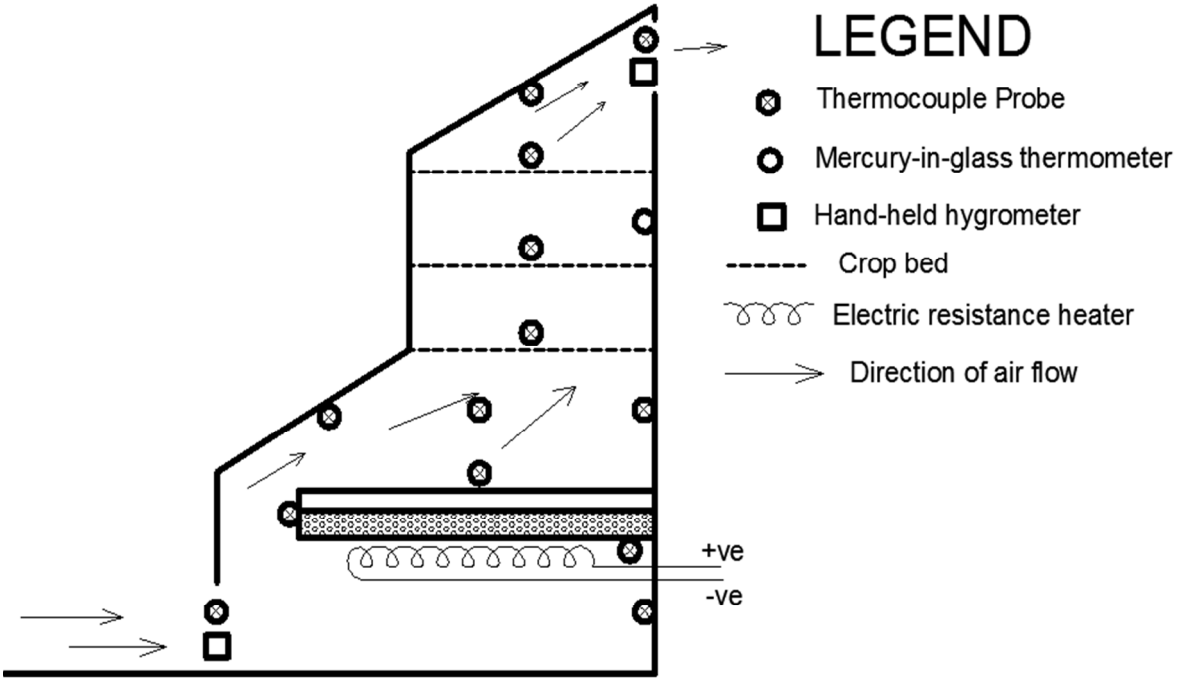

Figure 4 Schematic illustration of the laboratory dryer showing the locations of the temperature and relative humidity measuring sensors.

Air flow is induced by the difference between temperatures of air in the system components and ambient air (figure 4). From the fundamental principle that the buoyancy pressure head must be equal to the sum of all flow pressure losses between inlet and outlet, the underlying airflow equations is given by (Bala and Woods, 1994)

$$\beta\rho_a gH(\Delta T) = \Delta P_{bu} + \Delta P_{cu} + \Delta P_{db} + \Delta P_{vu} \qquad (2.1)$$

Resistive pressure within air passage components is given by:

$$\Delta P = \frac{1}{2}\left(\rho_i K_{bu,i} v_i^2 + \rho_p K_{cu} v_p^2 + \rho_o K_{vu} v_o^2\right) + K_{db} v_{db} \qquad (2.2)$$

where v_i is the average dryer inlet velocity, v_p is the average plenum velocity, v_{db} is the average drying cabinet velocity, and v_o is the average vent outlet velocity.

Combining the continuity of mass equation for the flow passage and equation (3.24) yields

$$\beta\rho_a gH\left(T_{f,o} - T_{f,i}\right) = \frac{1}{2}\left\{\rho_i K_{bu}\left(\frac{\rho_o A_o}{\rho_i A_i}\right)^2 + \frac{1}{2}\rho_p K_{cu}\left(\frac{\rho_o A_o}{\rho_p A_P}\right)^2 + \rho_o K_{vu}\right\} v_o^2 + \left(K_{db}\frac{\rho_o A_o}{\rho_{db} A_{db}}\right) v_o \qquad (2.3)$$

The terms on the RHS of equation (3.26) are pressure resistances due to contraction, bending, and expansion at inlet, expansion at the collector section, pressure resistance in the drying chamber, and bending and contraction at the dryer outlet, respectively. As the drying air leaves the back up heater enclosure, it passes through a narrow horizontal rectangular slot, resulting in contraction and pressure loss. In the collector, the drying air flows from a narrower cross-sectional area to a wider section at the exit from the collector resulting in air expansion and pressure loss.

The collector efficiency under solar heating, back up heating and hybrid heating modes are calculated using equations (2.4), (2.5), and (2.6), respectively

$$\eta_c = \frac{\dot{m} C_{p,a}(T_f - T_{f,i})}{A_{ab}\bar{S}_c} \qquad (2.4)$$

$$\eta_c = \frac{\dot{m} C_{p,a}(T_f - T_{f,i})}{(\bar{S}_c \text{譖}_{ab}) + \dot{Q}_{tm}} \qquad (2.6)$$

Average heat absorbed by thermal mass:

$$Q_{tm} = m_{ab}c_{ab}\left(T_{ab,av} - T_{fi}\right) + m_{rp}c_{rp}\left(T_{rp,av} - T_{fi}\right) \quad (2.7)$$

where $T_{ab,av} = \frac{1}{2}\left(T_{ab} + T_{ab\text{-}rp}\right)$ and $T_{rp,av} = \frac{1}{2}\left(T_{rp\text{-}bh} + T_{ab\text{-}rp}\right)$

Rate of change of flow exergy of air from dryer inlet to plenum exit is given by

$$\Delta\dot{\psi} = \dot{\psi}_2 - \dot{\psi}_1 = \dot{m}\left\{\left(h_2 - h_1\right) + T_o\left(s_2 - s_1\right) + \frac{1}{2}\left(v_2^2 - v_1^2\right) + g\left(z_2 - z_1\right)\right\} \quad (2.8)$$

where $h_2 - h_1$, $s_2 - s_1$, $z_2 - z_1$, and $v_2^2 - v_1^2$ are the changes in enthalpy, entropy, elevation, and the square of velocity of air through the dryer. The air entropy change is given by

$$s_2 - s_1 = c_v \ln\left(\frac{T_2}{T_1}\right) + R\ln\left(\frac{p_2}{p_1}\right) \quad (2.9)$$

Total entropy change equation for thermal mass is given as:

$$\left(\Delta S\right)_{tm} = m_{ab}c_{v,ab}\ln\left(\frac{T_{ab\text{-}rp}}{T_{ab}}\right) + m_{rp}c_{v,rp}\ln\left(\frac{T_{rp}}{T_{ab\text{-}rp}}\right) \quad (2.10)$$

In this study, we investigated the thermal buoyancy characteristics of a mixed mode natural convection solar crop dryer with back up heater. This was done by varying the plenum inlet and vent outlet openings. The investigations are currently based on a laboratory model of the dryer. It is expected that the attainment of an optimised plenum inlet opening to vent outlet opening ratio will help to provide a useful way of modeling the structure of a functional, and inexpensive, mixed-mode dryer with an adequate back up heating system.

3.0 Instrumentation

Pertinent system temperature measurements

A combination of hand-held instruments and sensors and a data logger were used to make and record measurements. Mercury-in-glass thermometers (250 ^{o}C maximum) with accuracy of ± 0.1^{o}C were also used for some temperature measurements. The relevant system temperatures were measured using K type copper-constantan thermocouples (temperature range: 0 to 200 ^{o} C). The output terminals from twelve thermocouples were connected to a thermocouple temperature logger (21X micrologger, Campbell Scientific; S/N 11552). The logger, which measures temperatures up to an accuracy of ± 0.01^{o}C was programmed using the 21X prompt sheet. The programme and, hence, data collected were stored on storage module SM 192 (S/N 11487). The temperatures were continuously monitored and logged out using the 21X Micrologger from Campbell Scientific Incorporation, U.S.A (see figure 5). The logger was programmed in the single channel mode to select an input to a channel every 5 minutes and the recorded data integrated to give the hour-by-hour values. Pertinent temperatures measured include the air inlet temperature, the heater housing floor temperature, the inner burner housing wall temperature, the rock bed bottom surface temperature, the rock pile-absorber interface temperature, the absorber top surface temperature, the inner plenum wall temperature, the plenum fluid temperature, and the air outlet temperature.

Figure 5 21X Micrologger, Campbell Scientific Incorporation, U.S.A

Air speed, relative humidity, atmospheric pressure and ambient temperature measurements

Wind speed, air inlet temperature, atmospheric pressure and air inlet relative humidity were measured with a weather center (model PCE-FWS 20 mounted at the test site).The air outlet temperature and relative humidity were measured with a portable Macronta LCD Indoor/Outdoor thermometer/hygrometer (CAT 63-867) in conjunction with a Vaisala H M34 humidity and temperature meter (measuring range: 0 – 100% RH and -4 to +140 ^{o}F). A Barnant 115 thermocouple (model number: 600-2810) was used to measure the rock bed-absorber interface temperature.

4.0 Method

Under no load conditions, the thermal buoyancy characteristics of the experimental dryer was investigated in three different heating modes namely, (1) solar heating, (2) back up heating, and (3) hybrid heating modes under varied plenum inlet area and vent outlet area scenarios. Measurements were made at intervals of twenty minutes between consecutive readings for all heating modes. Twenty seven (27) carefully planned tests were conducted with the plenum inlet gap to vent outlet gap combinations shown in table 1 for the three different heating modes in order to determine the optimum thermal drive characteristics of the dryer. Air velocities, temperatures, ambient relative humidity, collector efficiency, exergy rate of change, thermal mass entropy change and air mass flow rate were measured.

Table 1: Summary of the test conditions for dryer thermal buoyancy characteristic studies

Test condition	***Test mode***	***Vent width 1 (20 mm)***	***Vent width 2 (30 mm)***	***Vent width 3 (40)***
Plenum inlet opening 1 (20 mm)	Solar heating	1	2	3
	Burner heating	10	11	12
	Hybrid heating	19	20	21
Plenum inlet opening 2 (40 mm)	Solar heating	4	5	6
	Burner heating	13	14	15
	Hybrid heating	22	23	24
Plenum inlet opening 3 (60 mm)	Solar heating	7	8	9
	Burner heating	16	17	18
	Hybrid heating	25	26	27

The magnitude of data obtained from the tests is necessary in order to get a fairly accurate interpretation of the prevailing characteristics of the dryer. The tests 1 to 27 (see table 1) were conducted with the primary aim of examining the relative performance of the dryer operated with varied configurations of inlet and outlet openings. The tests under no load conditions were performed by adjusting the rectangular air inlet gap to three different positions. For each rectangular air inlet gap size chosen, the air outlet vent size was also adjusted to three different sizes while measuring temperatures, air flow rate and other performance characteristics for each of the three heating modes chosen. Results for tests numbers 1, 5, 9, 10, 14, 18, 19, 23, and 27 (see table 1) were plotted and analysed for interpretation in the following section.

5.0 Results and discussions

The objective of these set of tests was to establish the effects of the inlet and outlet areas as well as the various heating modes on thermal buoyancy (ventilation) through the dryer. The graphs show a plot of normalized thermal buoyancy property values against time for the tests presented. ***Solar heat charging mode:***

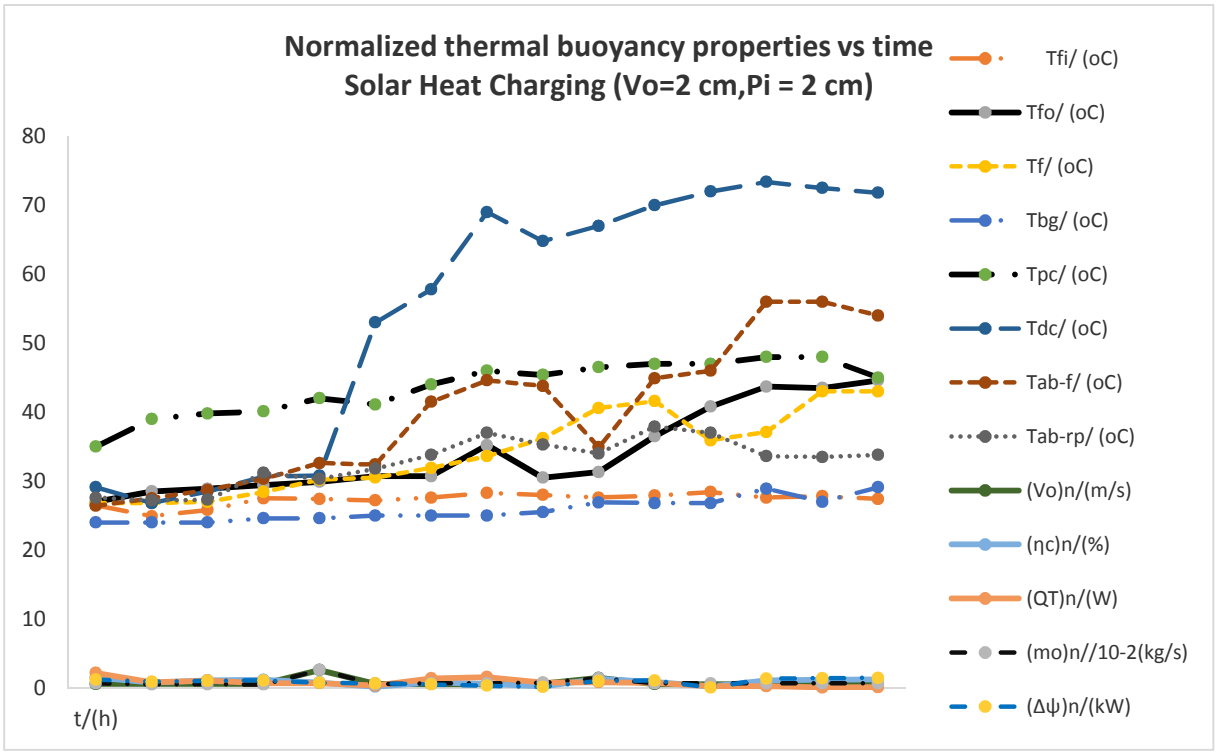

Figure 7 Thermal buoyancy properties versus time, solar heat charging (Vo = 2 cm, Pi = 2 cm)

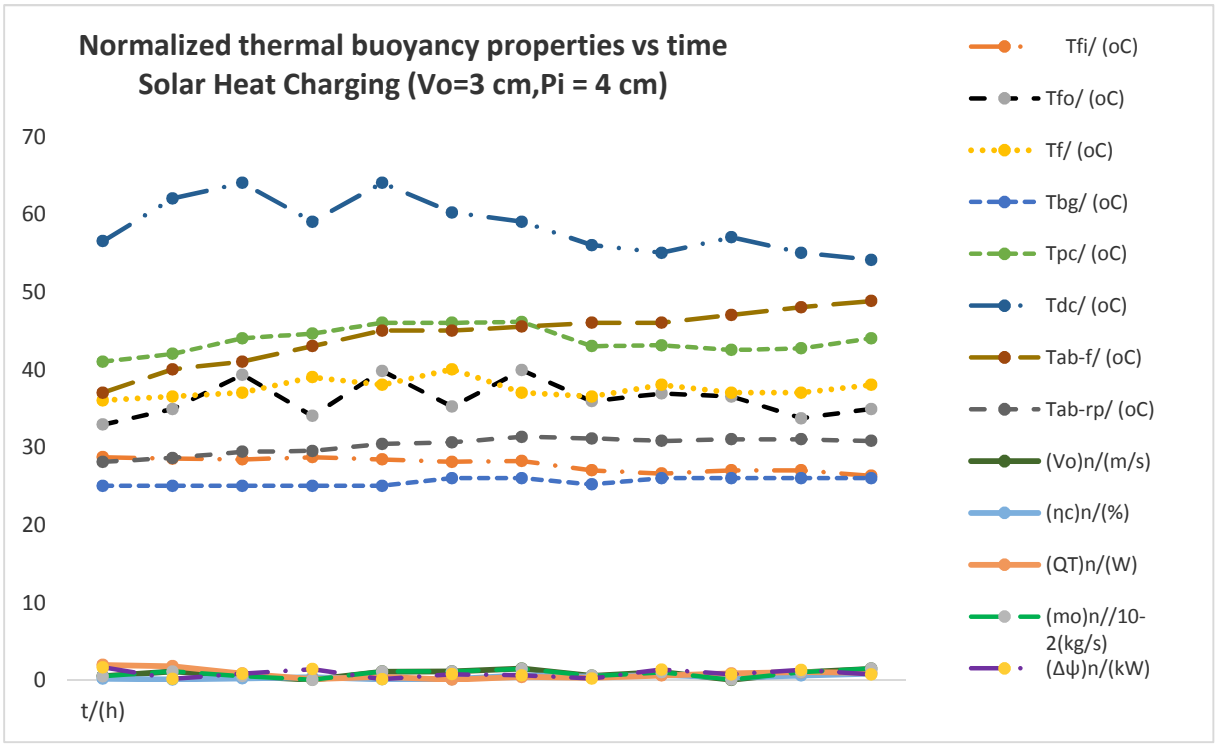

Figure 8 Thermal buoyancy properties versus time, solar heat charging (Vo = 3 cm, Pi = 4 cm)

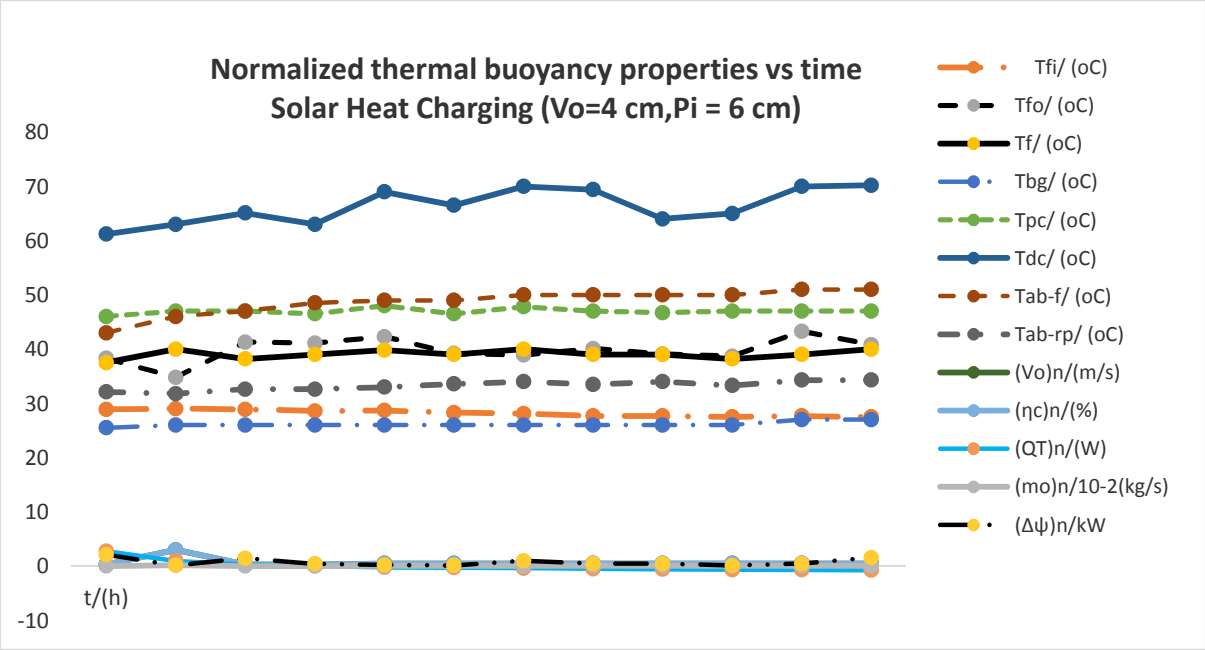

Figure 9 Thermal buoyancy properties versus time, solar heat charging (Vo = 4 cm, Pi = 6 cm)

Back up heat charging:

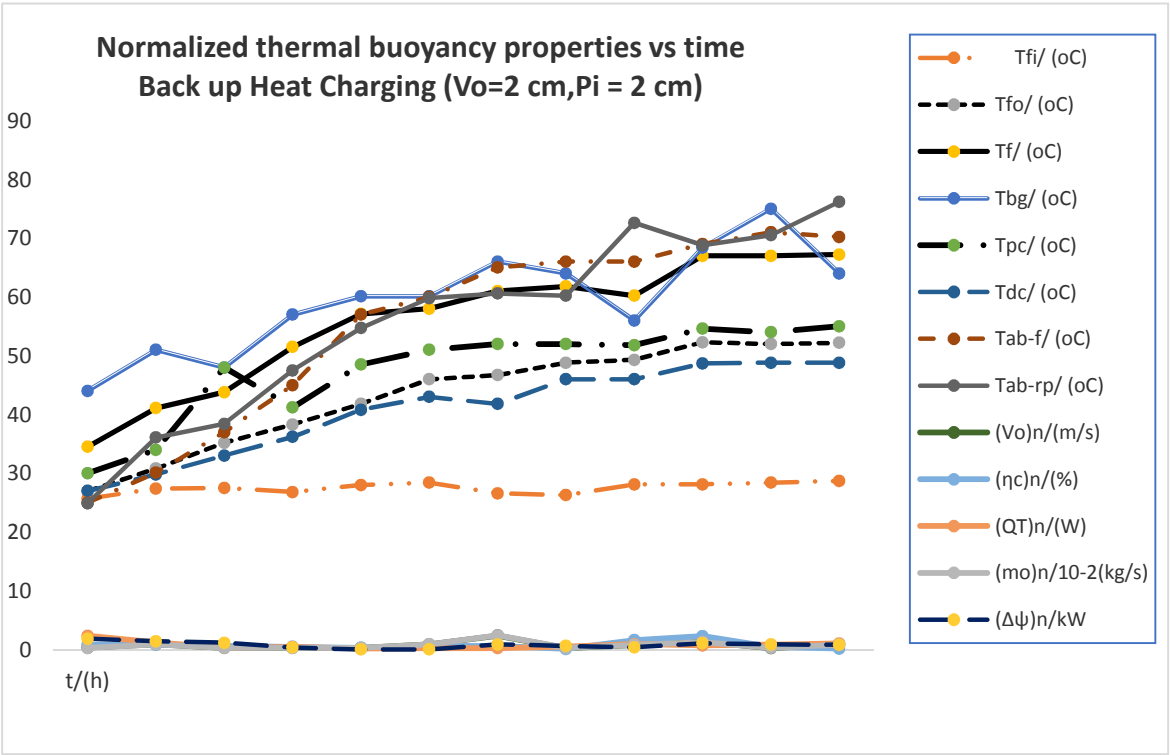

Figure 10 Thermal buoyancy properties versus time, back up heat charging (Vo = 2 cm, Pi = 2 cm)

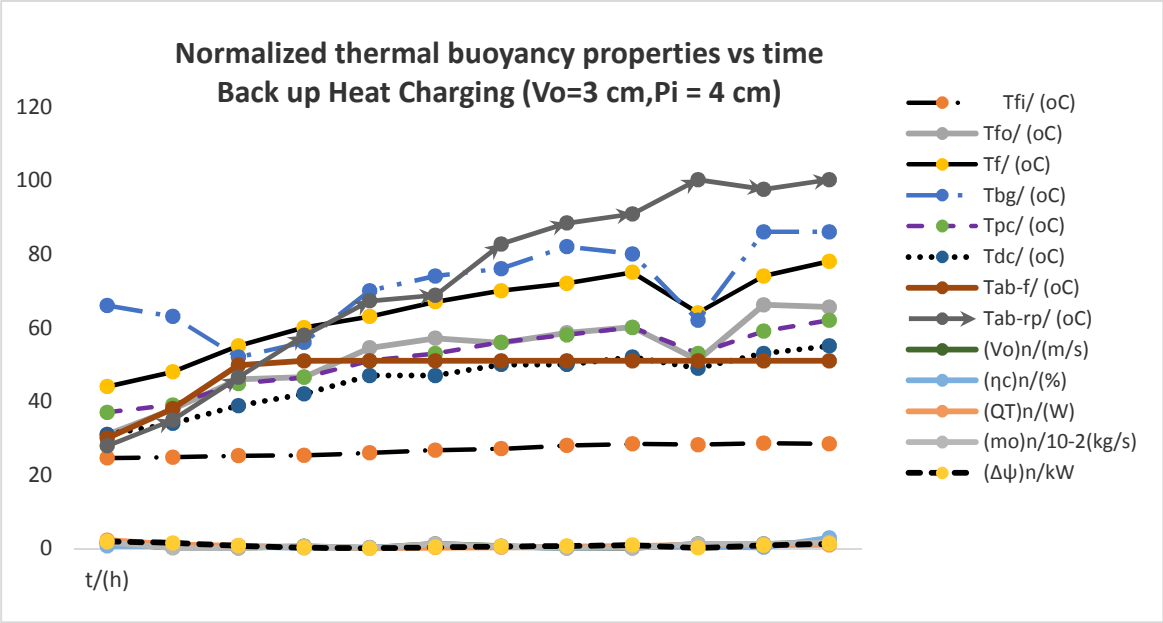

Figure 11 Thermal buoyancy properties versus time, back up heat charging (Vo = 3cm, Pi = 4cm)

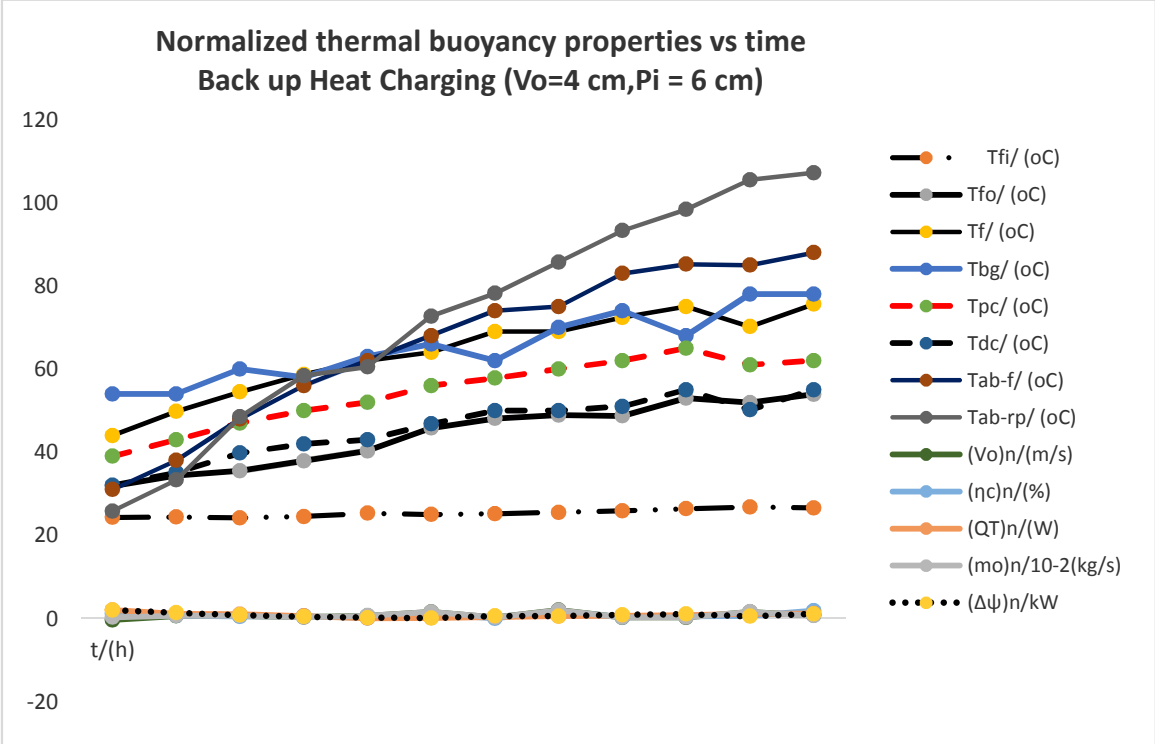

Figure 12 Thermal buoyancy properties versus time, back up heat charging (Vo = 3 cm, Pi =4 cm)

Hybrid heat charging:

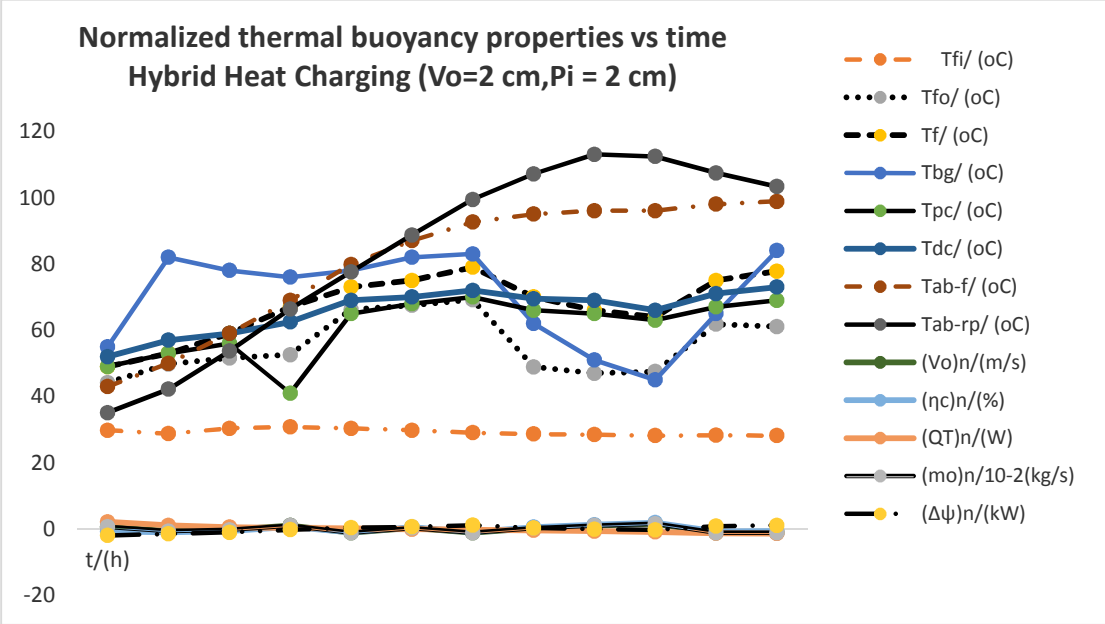

Figure 13 Thermal buoyancy properties versus time, hybrid heat charging (Vo = 2 cm, Pi =2 cm)

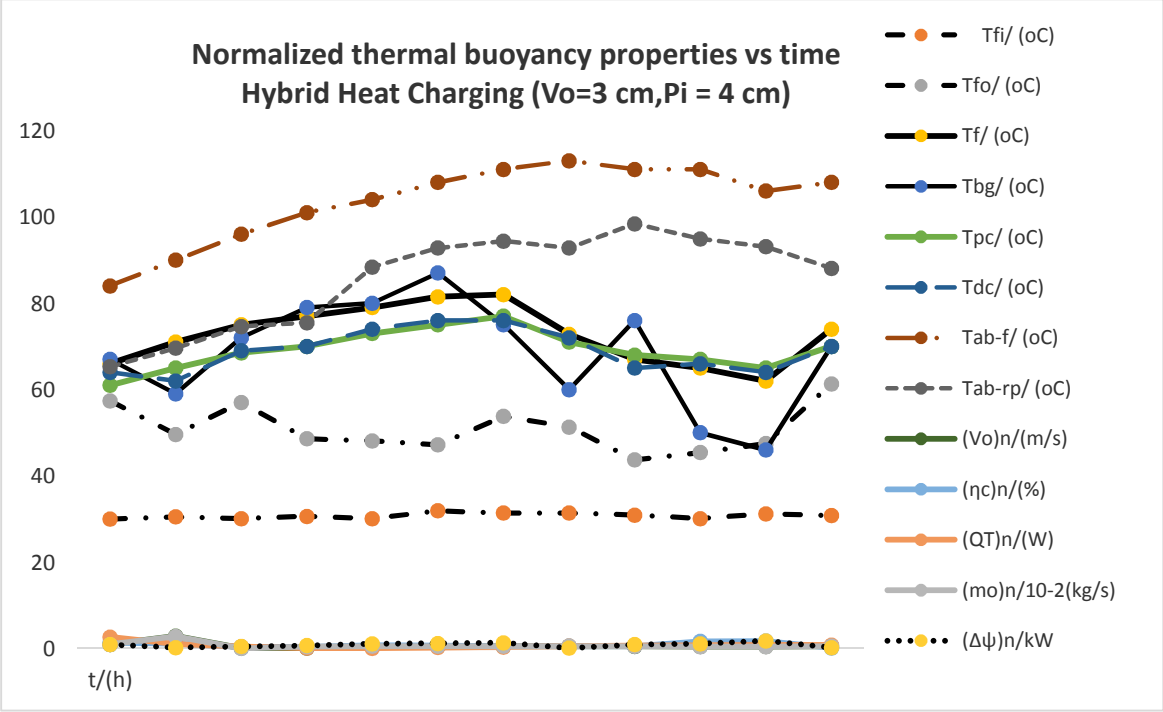

Figure 14 Thermal buoyancy properties versus time, hybrid heat charging (Vo= 3cm, Pi =4 cm)

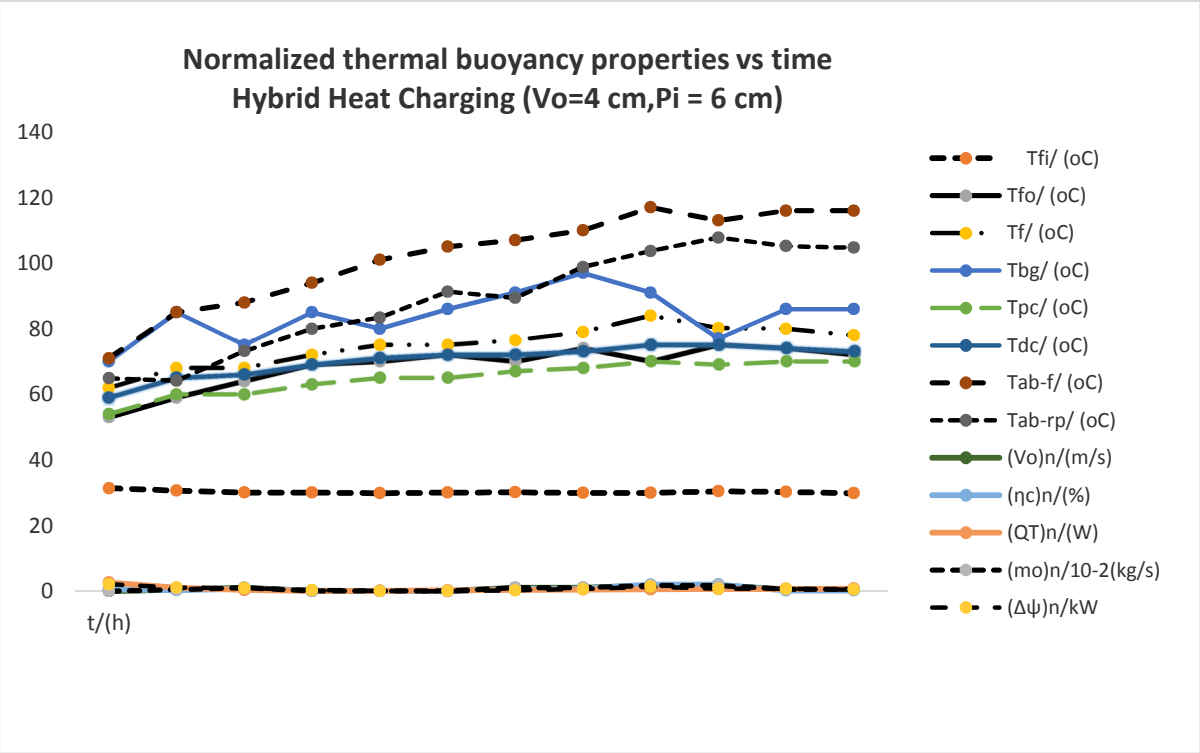

Figure 15 Thermal buoyancy properties versus time, hybrid heat charging (Vo = 4 cm, Pi =6 cm)

The Vx, Px notation used on the graphs of figure 7 to 15 are interpreted in the following legend:

LEGEND

V2:Vent outlet gap = 2 cm P2:Plenum inlet gap = 2cm

V3:Vent outlet gap = 3 cm P4:Plenum inlet gap = 4cm

V4:Vent outlet gap = 4 cm P6:Plenum inlet gap = 6cm

Table 2 Summary of results

Parameter range	Solar Heating			Back up Heating			Hybrid Heating		
	Test 1, V2,P2	*Test 5, V3,P4*	*Test 9, V4,P6*	*Test10, V2,P2*	*Test14, V3,P4*	*Test18, V4,P6*	*Test19, V2,P2*	*Test23, V3,P4*	*Test27, V4,P6*
T_{fi}/ (°C)	24.9-28.4	25.9-28.7	27.5-29	25.7-28.7	24.6-28.6	24.3-26.8	28.2-30.8	30-31.9	29.9-31.4
T_{fo}/ (°C)	27-45.7	32.2-39.9	34.8-43.3	27-52.3	31-66.2	31.8-53.9	44.2-69.2	43.7-61.3	53-74
T_f/ (°C)	26.8-43	36-40	37.5-40	34.5-67.2	44-78	44-75.6	49-77.8	66-82	62-84
T_{bg}/ (°C)	24-29	25-26	25.5-27	44-68.4	52-86	54-78	51-84	46-87	70-97
T_{ab-f}/ (°C)	26.4-56	37-49	43-51	25-71	30-51	31-88	43-98.8	84-111	71-117
T_{rp-ab}/ (°C)	27.2-37.9	28.1-31.8	31.8-34.3	24.9-76.2	27.9-100.2	25.8-107.2	35.1-113	65.3-98.4	64.2-107.8
T_{rp-f}/ (°C)	25.7-38.6	26-31	30.1-33	89-201	138-243	114-242	114-242	116-240	150-241
T_{pc}/ (°C)	35-48	41-46.1	46.5-48	30-55	37-62	39-65	41-70	61-77	54-70
T_{dc}/ (°C)	26.8-77.5	54.1-64	61.2-70.2	27-48.8	31-55+	32-55	52-73	62-76	59-75
ϕ_i/ (%)	56-70	57-75	54-64	69-83	67-87	73-86	57-67	51-60	52-57
ϕ_o/ (%)	62-76	52.7-72	50.2-60.2	77.7-93.7	66.6-82.7	56.3-81.6	43-63.8	31.2-51.3	45-52.7
V_o/ (m/s)	0.518-2.594	0.040-1.456	0.270-0.478	0.265-2.387	0.140-1.828	0.239-2.02	0.203-1.612	0.077-2.859	0.028-1.816
η_c/ (%)	0.178-1.514	0.083-0.194	0.27-2.99	0.187-1.610	0.159-0.745	0.031-1.869	0.571-1.98	0.113-1.739	0.019-2.079
Q_T/ (W)	0.067-2.188	0.055-1.942	0.047-2.757	0.188-2.367	0.098-2.284	0.043-2.028	0.029-2.179	0.067-2.655	0.0815-2.669
m_o/ [10^{-2}kg/s]	0.515-1.413	0.017-1.47	0.017-0.194	0.295-2.401	0.165-1.687	0.287-1.943	0.329-1.103	0.024-2.797	0.025-1.813
Patm/ (hPa)	979.1-982	976.6-978.1	978.7-980	979.2-981.7	981.3-981.6	981.1-981.9	978-980.3	979.7-980.5	979.7-982.0
Δψ/(kW)	0.043-1.449	0.164-1.637	0.110-2.124	0.034-1.870	0.015-1.945	0.091-2.018	0.034-1.926	0.092-1.758	0.0647-2.144

Table 2 shows an overview of ambient, inlet and outlet air and dryer component conditions in the no-load trials for the different configurations considered under the three heating modes. When comparing the performance of different configurations, the air outlet velocity, air mass flow rate, air outlet relative humidity, rate of flow exergy, heat absorbed by thermal mass and collector efficiency were used as the key parameters for comparative analysis.

The levels of inlet air relative humidity ranged from 54% to 75%, for solar heating mode; 67% to 87% for back up heating mode; and 52% to 67% for hybrid heating mode with mean ambient air temperatures varying between 297.9 K and 302K; 297.3 K and 301.7 K; and 301.2 K and 304.9 K for solar, back up, and hybrid heating modes respectively. Atmospheric pressure values recorded at the test site over the entire period of experimentation ranged between 975.7 hPa and 985.4 hPa with the minimum and maximum values occurring on July 04, 2012 (for test 4, see table 1) and July 06, 2012 (test 24, see table 1 for test configuration) respectively.

Minimum and maximum temperature difference values (i.e. the average difference between vent outlet air temperature and dryer inlet air temperature, $\Delta T = T_{fo} - T_{fi}$) for V2, P2 under solar, back up and hybrid heating modes (i.e. tests 1, test 10 and test 19) are 2.1 and 17 ^{o}C; 1.3 and 23.6 ^{o}C; and 16 and 38.4 ^{o}C, respectively. Minimum and maximum temperature difference values for V3, P4 under solar, back up and hybrid heat charging modes (i.e. test 5, test 14 and test 23) are 6.3 and 11.2 ^{o}C; 6.4 and 37.6 ^{o}C; and 13.7 and 29.4 ^{o}C respectively. The values for V4, P6 under the three heating modes (i.e. test 9, test 18, and test 27) are 7.3 and 14.3 ^{o}C; 7.5 and 27.1^{o}C; and 23.1 and 42.6 ^{o}C, respectively. The average temperature difference between dryer inlet air and vent outlet air is directly proportional to thermal buoyancy through the dryer. Leon et al. (2002) reported that a temperature difference of at least 10 K is required for effective drying. With the exception of V3, P4 under back up heating mode, the average temperature differences for V4, P6 are relatively higher under all heating modes examined. A higher temperature difference value (between dryer inlet and dryer outlet air) causes a proportional increase in air mass flow rate, hence, increasing dryer efficiency. For instance, under solar heat charging mode (flow configuration V2, P2), the maximum dryer inlet and outlet air temperature difference is 17.3 ^{o}C and the maximum mass flow rate and collector efficiency values are 1.413×10^{-2} kg/s and 1.41%, respectively. However, considering the hybrid mode (flow configuration V4, P6), the maximum temperature difference value of 23.1 ^{o}C was obtained giving rise to maximum air mass flow rate and collector efficiency values of 1.81×10^{-2} kg/s and 2.08 %, respectively.

For the solar mode of operation (test 1, test 5, and test 9) the measured average plenum fluid temperatures (T_f) are relatively higher than the average dryer inlet air temperatures. It was found that there was significant difference between the plenum and ambient temperatures during the day (temperature difference ranges of 1.9 to 14.6 ^{o}C for test 1; 10.1 to 11.3 ^{o}C for test 5; and 10 to 11^{o}C for test 9, respectively) which indicates that the insulation cover over the solar collector was effective in limiting heat losses from the plenum fluid to the ambient. The magnitude of the plenum fluid temperature indicates the quantity of heat energy the fluid transfers to the drying chamber for the purpose of drying.

The calculated thermal energy stored by the *thermal mass* during solar heat charging (this was done using equation (2.7)) ranges from 0.0086 MJ to 0.1457 MJ whereas the range of values for back up heating and hybrid heating are 0.0918 to 0.4697 MJ and 0.1154 to 0.9454 MJ, respectively. The corresponding collector efficiency values recorded ranged from 0.083 to 2.99% for solar heating, 0.031 to 1.87% for back up heating, and 0.019 to 2.08% for hybrid heating, respectively. Clearly, the thermal energy stored in solar heating mode (equivalently 7.20 W to 121.4 W) is inadequate to sustain drying at night time or in periods of inclement weather. This apparently indicates the need for back up heating. The heat charging rate regime recorded for back up heating mode (equivalently 102 to 521.9 W), obviously provides a more effective means of augmenting the unsteady solar heating mode. A hybrid heating mode (with equivalent heat charging rate of 128.2 to 1050.4 W) offers a practically feasible way of dealing with low, inconsistent solar radiation experienced in extremely poor weather such as the June to September period in Ghana which is characterized by intense raining activity with a lot of cloudy weather. These conditions indicate that drying will not be effective on some days if back up heating is not employed. The relatively low collector efficiency values recorded in the solar heat charging mode coupled with the comparatively low air mass flow rates (0.00017 to $1.47\text{x}10^{-2}$ kg/s) recorded, further reveals the need for back up heating. In back up heating mode, tests 10, 14, and 18 recorded minimum and maximum normalized mass flow rate values of 0.00295 and 0.02401 kg/s; 0.00165 and 0.0687 kg/s; and 0.00287 and 0.01943 kg/s respectively. The corresponding minimum and maximum air mass flow rate values for tests 19, 23, and 27 are 0.00329 and 0.01103 kg/s; 0.00024 and 0.02797 kg/s; and 0.00025 and 0.01813 kg/s respectively. Enibe (2002) observed a maximum flow rate of 0.058 kg/s for natural convection solar air heating systems.

The vent outlet air velocity, air mass flow rate, and collector efficiency range of values recorded for test configuration V4, P6 under each of the heating modes show significantly improved conditions relative to the other configurations dealt with (see table 1).

The temperature of the floor of the back up heater compartment recorded temperature values of 24 to 29 ^{o}C for solar heating mode, 44 to 86 ^{o}C for back up heating mode, and 46 to 87 ^{o}C for hybrid heating mode. The range of values for solar heat charging mode is obviously lower than that for back up and hybrid heating modes. The difference in temperature between the back up heater compartment floor and the ambient throughout the solar heat charging series of tests is insignificant. Thus, the floor did not significantly contribute to air heating in solar heat charging mode. It can, however, be seen that the back up heater compartment floor contributed tremendously to thermal drive through the dryer in the back up heating and hybrid heating modes respectively since temperature difference ranges recorded were 18.3 to 39.7 ^{o}C for test 10; 27.4 to 57.4 for test 14; 29.7 to 51.2 ^{o}C for test 18; 22.8 to 53.2 ^{o}C for test 19; 16 to 55.1 ^{o}C for test 23; and 40.1 to 65.6^{o}C for test 27. The range of temperature values recorded for the plenum cover glass for the tests under solar, back up, and hybrid heating ranged from 35 to 70.2 ^{o}C, 30 to 65 ^{o}C, and 41 to 77 ^{o}C respectively. Also, the range of drying chamber cover glass temperature values for solar heating, back up heating and hybrid heating modes are 26.8 to 77.5^{o}C, 27 to 55^{o}C, and 52^{o}C, respectively. These results agree closely with the results reported by Singh and Kumar (2011)

for natural convection within an insolation range of 300 to 550 W/m^2.

The exergy analysis conducted on the air from dryer inlet to plenum exit give the minimum and maximum normalized rate of change of exergy values as 0.043 and 1.449 kW; 0.164 and 1.637 kW; 0.110 and 2.124 kW; 0.034 and 1.870 kW; 0.015 and 1.945 kW; 0.091 and 2.018 kW; 0.034 and 1.924 kW; 0.092 and 1.758 kW; and 0.0647 and 2.144 kW for tests 1, 5,9, 10, 14, 18, 19, 23, and 27 respectively. These results show that the exergy rate of the dryer increases with increased heating effect (solar being the lowest and hybrid the highest). In comparison with the range of collector efficiency values recorded for the three heating modes, it can be concluded that as the system exergy increases the collector efficiency increases. Therefore, the performance of the system can be improved by adopting a heating effect that optimises exergy. It can further be concluded that the performance of the system can be improved by adopting a design that minimizes heat losses since that will increase the ***exergy*** of the system.

6.0 Conclusions

The experiments conducted on the laboratory model of a mixed mode natural convection solar crop dryer with back up heater (MMNCSCDBH) have shown that for test configurations V2, P2, and V3, P4 in each of the three heating modes, the air flow through the dryer is inadequate and that temperatures in the system components become high giving rise to relatively high plenum inlet temperatures and relatively low collector efficiencies.

Exergy analysis results show that the exergy rate of change of the dryer increases with increased heating effect (solar being the lowest and hybrid the highest). In comparison with the range of collector efficiency values recorded for the three heating modes, it can be concluded that as the exergy of the system increases the collector efficiency increases. Therefore, the performance of the system can be improved by adopting a heating effect that optimises exergy. It can further be concluded that the performance of the system can be improved by adopting a design that minimizes heat losses since that will increase the ***exergy*** of the system.

In solar heating mode it was noticed that the thermal energy stored was not sufficient enough to sustain drying at night and also in inclement weather and hence the need for back up heating.

At a test configuration of V4, P6 in all heating modes, comparatively high mass flow rates were recorded with comparatively high air heater efficiency values. The trend of results reveals that test configuration V4, P6 optimises the thermal performance of the dryer. For design purposes a plenum inlet gap to vent outlet gap ratio of 1.5:1 optimises air flow through the dryer.

7.0 ACKNOWLEDGEMENT

The material support rendered by the Department of Mechanical Engineering, KNUST, Kumasi, and the immense technical supervision offered by Prof F.K. Forson of the same Department, is gratefully acknowledged.

REFERENCES

Dapaah, S.K. 1991. *Evaluation of Post-production Systems for Cereals in Ghana*. Phase One Report Prepared for National Energy Board (now Ministry of Mines and Energy), Ghana, October, 1991

Enibe, O.S., 2002. Performance of a natural circulation solar air heating system with phase change material energy storage. Renewable Energy 27, 69–86.

Leon, M.A., Kumar, S. and Bhattacharya, S.C. 2002. A comprehensive procedure for performance evaluation of solar food dryers. I.: Renewable and sustainable energy reviews, 6 (2002) 367 – 393.

Madhlopa, A., Ngwalo, G., 2006. Solar dryer with thermal storage and biomass-backup heater. Solar Energy 81(2007), 449 – 462.

Ratti, C., Mujumdar, A.S., 1997. Solar dryer of foods: modelling and numerical simulation. Solar Energy 60, 151–157.

Simate I.N. (2003), Optimization of mixed-mode and indirect-natural convection solar dryers, Renewable Energy, 28, 435–453.

Soponronnarit, S., 1995. Solar drying in Thailand. Energy for Sustainable Development 2, 19–25.